EXPERIMENTAL ANALYSIS AND OPTIMIZATION OF EDM PROCESS PARAMETERS THROUGH MODELING OF MATERIAL REMOVAL AND ELECTRODE WEAR BEHAVIOR

Adelina-Alina Han[1], Dinu-Valentin Gubencu[2] and Liliana-Georgeta Tulcan[3]
[1]Politehnica UniversityTimisoara, Romania, *Corresponding author*, ORCID No.0000-0002-4003-6273, adelina.han@upt.ro
[2]Politehnica UniversityTimisoara, Romania, ORCID No. 0000-0001-9512-7757, dinu.gubencu@upt.ro
[3]Politehnica University Timisoara, Romania, ORCID No. 0000-0002-4599-4454, liliana.tulcan@upt.ro

ABSTRACT: This paper presents an experimental approach to analyze and optimize the Electrical Discharge Machining (EDM). The study's core methodology involves developing a model of the process to determine the functional relationship between the input parameters and the resulting Material Removal Rate (MRR) and Tool Wear Rate (TWR).The research demonstrated that impulse energy (W_i) is the most influential factor on MRR, while electrode diameter (D_e) is the most significant for TWR. It was also observed that brass electrodes have a higher wear rate than copper ones, due to their inferior electrical and thermal conductivity. The surface analysis confirmed that brass electrodes produce greater roughness, while copper electrodes provide superior surface quality. The study established two optimal parameter configurations for maximizing performance. For the brass electrode, the optimal combination was at a W_i of 0.45 J and a D_e of 10 mm, resulting in an MRR of 114.58 mm^3/min and an TWR of 5.92%. For the copper electrode, the optimal settings were a W_i of 0.60 J and a D_e of 8.59 mm, which led to an MRR of 102.24 mm^3/min and an TWR of 4.98%. The results highlight the importance of parameter optimization to ensure process productivity and efficiency.

KEYWORDS: electrical discharge machining, full factorial experiment, material removal rate, electrode wear rate

1. INTRODUCTION

In recent years, the demand for new materials that are difficult to machine with conventional methods has grown in all industrial sectors Electrical discharge machining (EDM) has become an essential solution for these conductive materials because it enables the precise machining of complex shapes without direct contact or deforming forces. This technology is particularly important for the tool, die, and parts manufacturing industries that require high hardness and resistance [1, 2, 3].

Recent studies in the field of EDM have analyzed various aspects, from the development of prediction models for material removal rate and electrode wear, to the effects of using powders in the dielectric fluid and the influence of input parameters on surface quality. These studies have also highlighted the importance of factors such as electrode polarity and material, showing that they can significantly influence the process's performance [4, 5].

During the EDM process material is removed primarily through the thermal effect of electrical discharges successively generated between the electrode and the workpiece (Figure 1). A small gap (the erosive gap) between the surfaces of these two objects is filled with a liquid dielectric medium (hydrocarbons, deionized water etc.). Material removal from the workpiece is the result of the cumulative actions of electrical discharges, the relative movements of the electrodes, and the debris evacuation processes. During the machining process, the electrode also experiences wear, which is the result of material removal [6, 7].

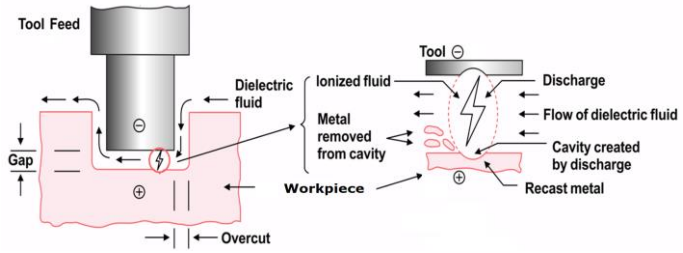

Figure 1. The principle of EDM processing

The main performance parameters in the EDM process are MRR (material removal rate), TWR (tool wear rate), and surface quality. MRR measures the workpiece erosion rate and consequently the machining speed, while TWR directly influences the geometry and accuracy of the machined cavity through continuous changes in electrode profile during machining. Surface quality is a complex characteristic that includes roughness, recast layer thickness, micro-crack density, and heat-affected zone extent [2, 4, 7].

EDM process parameters are divided into two categories: electrical parameters (discharge voltage, peak current, pulse duration and interval, polarity) and non-electrical parameters (dielectric fluid flushing, workpiece and electrode movement).

Discharge voltage directly influences the spark gap size and overcut, while increased current raises both MRR and TWR, negatively affecting machining accuracy. Pulse-on time determines the generated energy and consequently the MRR, while pulse-off time allows debris evacuation from the gap between electrode and workpiece, ensuring stable machining conditions [6, 8, 9].

The dielectric fluid must have high dielectric strength and good flushing capability, and electrode and workpiece movement improves evacuation conditions, resulting in higher MRR and better surface roughness [8, 10].

The electrode material is a critical factor in the electrical discharge machining (EDM) process, as its physical properties directly influence machining performance. The most important aspects to consider are the electrical and thermal conductivity, as well as the material's melting point [11].

This paper focuses on developing an empirical model to capture the relationship between the input parameters of Electrical Discharge Machining (EDM) and its critical performance metrics, namely Material Removal Rate (MRR) and Tool Wear Rate (TWR). By analyzing how changes in process parameters affect machining efficiency and tool degradation, the study aims to provide a predictive framework that can guide the optimization of EDM operations.

2. MATERIALS AND METHODES

The experimental methodology employs an empirical modeling approach based on quantitative data acquisition, utilizing a black-box input-output framework. This approach deliberately avoids detailed phenomenological analysis, focusing on establishing statistically significant correlations between objective functions and influence factors through mathematical-statistical methods. The experimental design incorporates a full factorial framework with three critical influence factors to derive regression models describing functional relationships between examined variables.

The workpiece material is OL60/E335 steel, with a Brinell hardness of 160 HB, supplied by Antera Steel, Romania, which is commonly used for the fabrication of wear-resistant machine components.

The experiments were performed using an EROSIMAT C machine equipped with a pulse generator. The machining process was performed through immersion, using a paraffin-based dielectric fluid specifically engineered for die-sinking EDM. This was conducted under conditions of direct polarity (+electrode, -workpiece), with the dielectric fluid maintained at a pressure of 20 kPa.

The characterization of the EDM process was performed by determining two objective functions:

- MRR [mm^3/min]: Material Removal Rate which quantifies the volume of material removed from the workpiece per unit of time;
- TWR [%]: Tool Wear Rate, defined as the ratio between the volume of material lost from the electrode during the EDM process and the volume of material removed from the workpiece

Material Removal Ratewas chosen because this parameter reflects the speed and efficiency of material removal, directly influencing process productivity, optimization of machining costs and the proper selection of technological parameters [8].

Studying the Tool Wear Rate is important because it indicates the degree of electrode wear during EDM process, influencing the dimensional accuracy of the workpiece, the costs and frequency of electrode replacement, as well as the stability and repeatability of the process [9, 10].

For determining the two objective functions, the following relations were used:

$$MRR = \frac{V_w}{t} \qquad TWR = \frac{V_e}{V_w} \times 100 \tag{1}$$

where:

- V_w[mm^3]: volume of material removed from the workpiece;
- V_e[mm^3]: volume of electrode material erodeted;
- t [min]: processing time.

Since the electrodes have a cylindrical shape, V_e and V_w were determined using the formulas:

$$V_e = \pi \cdot \frac{D_e^2}{4} \cdot h_e \qquad V_w = \pi \cdot \frac{D_w^2}{4} \cdot h_w \tag{3}$$

where:

- D_e[mm]: diameter of the electrode;
- h_e[mm]: thickness of material lost from the electrode;
- D_w[mm]: diameter of the cavity (material removed from the workpiece);
- h_w[mm]: depth of material removed from the workpiece.

The 3 influence parameters chosen for carrying out the experimental programmeare:

- Impulse Energy W_i [J];
- Electrode Diameter D_e [mm];
- Electrode Material Mat_EL[-].

Copper (Cu) is a classic material used in EDM due to its high electrical and thermal conductivity, which ensures reduced electrode wear and a high machining speed. At the same time, copper electrodes are durable and wear-resistant, making them ideal for precision work and fine surface finishes, although their mechanical processing is more difficult and costly. In contrast, brass (an alloy of Cu and Zn) is preferred in many applications due to its excellent machinability and lower cost compared to copper, although it has lower electrical conductivity and faster wear [2, 3].

The parametric ranges for each experimental factor (Table 1) were established through comprehensive consideration of relevant research conducted by multiple investigators, industrial expertise, and preliminary experimental investigations undertaken by the present research team.

Table 1. Experimental levels for the influence factors

Factors	Impulse Energy W_i [J]	Electrode Diameter D_e [mm]	Electrode Material Mat_EL [-]
	$X_1 \equiv W_i$	$X_2 \equiv D_e$	$X_3 \equiv$ Mat_EL
Central Point (0)	0,4	8	-
Range of Variation	0,2	2	-
Lower Level (-1)	0,2	6	Brass
Higher Level (+1)	0,6	10	Copper

To ensure valid and comparable results, each machining test was run for a duration of 5 minutes. This period was considered sufficient to achieve a steady state of the erosion process, thus allowing for a reliable and representative measurement of the objective functions.

3. RESULTS AND DISCUSSIONS

For modeling the action of a number of p influence factors selected, x_j, on a performance characteristic, y, by means of a 2^p full factorial experiment, the experimental resultsare used to find the constants, b_0, b_j, b_{jk}, of the polynomial [12, 13]:

$$y = b_0 + \sum_{j=1}^{p} b_j x_j + \sum_{j,k=1,\ j\neq k}^{p} b_{jk} x_j x_k \quad (4)$$

This experimental design enables the acquisition of a high-precision model from a minimal number of trials, thereby reducing investigation costs.

3.1 Experimental Design and Measured Results

Adhering to the principles of full factorial design, the experimental matrix (Table 2) was created to include all possible factor-level combinations [13]. To ensure a robust estimation of experimental error, two additional runs were conducted at the central point for the impulse energy and electrode diameter parameters, using a copper electrode. The results for all three objective functions are detailed in Table 2.

For processing, analyzing, and plotting the experimental data, the statistical dedicated software Minitab® 17 was applied.

Measurements of the electrode diameter, the cavity diameter, the depth of the material removed from the workpiece and the material lost from the electrode were performed using a Mitutoyo caliper with a precision of 0.01 mm.

Table 2. Matrix and results of the 2^3 full factorial experiments

Run No i	Influence Factors						Objective Functions	
	A : W_i		B : D_e		C : Mat_EL		MRR [mm^3/min]	TWR [%]
	Coded	[J]	Coded	[mm]	Coded	[-]		
1	-1	0,2	-1	6	-1	Brass	108,04	6,65
2	+1	0,6	-1	6	-1	Brass	148,58	7,40
3	-1	0,2	+1	10	-1	Brass	93,12	5,02
4	+1	0,6	+1	10	-1	Brass	126,84	6,49
5	-1	0,2	-1	6	+1	Copper	86,21	5,20
6	+1	0,6	-1	6	+1	Copper	119,39	6,50
7	-1	0,2	+1	10	+1	Copper	73,14	3,38
8	+1	0,6	+1	10	+1	Copper	92,54	4,09
9	0	0,4	0	8	-1	Copper	81,45	3,71
10	0	0,4	0	8	-1	Copper	78,27	3,69

3.2 Analysis of the Material Removal Rate

The effects of selected input parameters on the MRR are shown in Figure 2. It can be observed that increasing the impulse energy, W_i, ensure an increase of the MRR. An increase in pulse energy directly correlates with a higher MRR. A greater thermal energy per pulse generates a more expansive and intense plasma channel, which results in the melting and vaporization of a larger volume of material with each discharge. Consequently, a higher processing rate is achieved per unit of time.

Increasing the electrode diameter leads to a decrease in the MRR (Figure 2). This can be attributed to the fact that the smaller diameter electrode (6 mm) concentrates the same impulse energy onto a more restricted contact surface. This leads to a higher power density and, implicitly, to a greater temperature at the point of discharge. A higher temperature generates more intense melting and vaporization of the material, which leads to a larger volume of material being removed per unit of time.

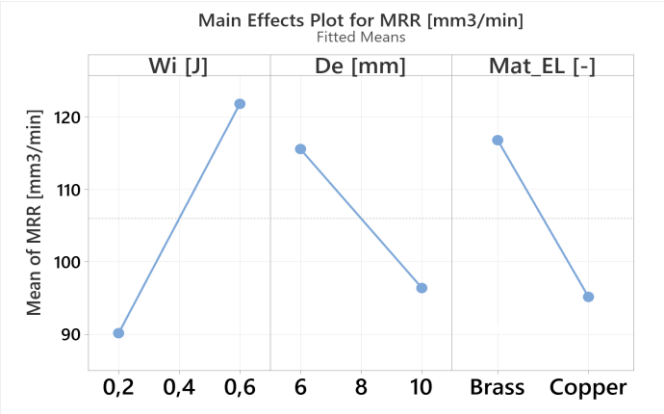

Figure 2. Main effects plot for MRM

The brass electrode yields a higher MRR than the copper electrode (Figure 2). Due to its lower thermal conductivity compared to pure copper, brass allows for less heat dissipation during the electrical discharge. This property facilitates a more efficient concentration of thermal energy in the erosion zone, intensifying the melting and vaporization process, which leads to a superior MRR.

The regression coefficients, which show the influence of the three selected factors and their interactions on MRR, were also calculated using the sofware (Table 3). The sign and value of each coefficient indicate the direction and amplitude of the corresponding influence.

Table 3. Calculated values of regression coefficients for MRR

Coeff.	Value	Coeff.	Value
b_0	105,983	b_{12}	-2,575
b_1	15,855	b_{13}	-2,710
b_2	-9,572	b_{23}	-0,407
b_3	-13,163		

To determine which factors have a statistically significant impact on MRR, an analysis of variance (ANOVA) was used (Figure 3). The results show that all influence factors have a significant effect on MRR (p-value < 0.05, at a 95% confidence level). In contrast, all interaction effects are insignificant (p-value > 0.05) and can therefore be omitted from the final model [12].

The hierarchy of factors, ranked by their influence, indicates that pulse energy is the most significant factor, followed by electrode material (Figure 4).

Source	DF	Adj SS	Adj MS	F-Value	P-Value
Model	7	5335,06	762,15	137,18	0,007
Linear	3	4130,12	1376,71	247,80	0,004
Wi [J 10-3]	1	2011,05	2011,05	361,98	0,003
De [mm]	1	733,06	733,06	131,95	0,007
Mat_EL [-]	1	1386,01	1386,01	249,48	0,004
2-Way Interactions	3	113,13	37,71	6,79	0,131
Wi [J 10-3]*De [mm]	1	53,05	53,05	9,55	0,091
Wi [J 10-3]*Mat_EL [-]	1	58,75	58,75	10,58	0,083
De [mm]*Mat_EL [-]	1	1,33	1,33	0,24	0,673
Curvature	1	1091,82	1091,82	196,52	0,005
Error	2	11,11	5,56		
Lack-of-Fit	1	6,06	6,06	1,20	0,471
Pure Error	1	5,06	5,06		
Total	9	5346,18			

Figure 3. ANOVA for MRRE

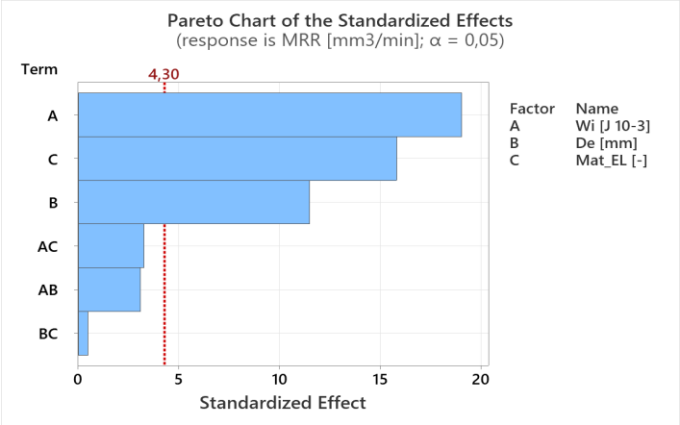

Figure 4. Hierarchy of factors effects for MRRE

Based on the statistical significance of the regression coefficients, the regression equation of the empirical models is:

$$MRR = 105{,}98 + 15{,}85\ Wi - 9{,}57\ De - 13{,}16\ Mat\_EL \quad (5)$$

Three-dimensional response surface plots [15] are employed to graphically illustrate the developed empirical models, as presented in Figure 6 for the brass electrode and Figure 6 for the copper electrode.

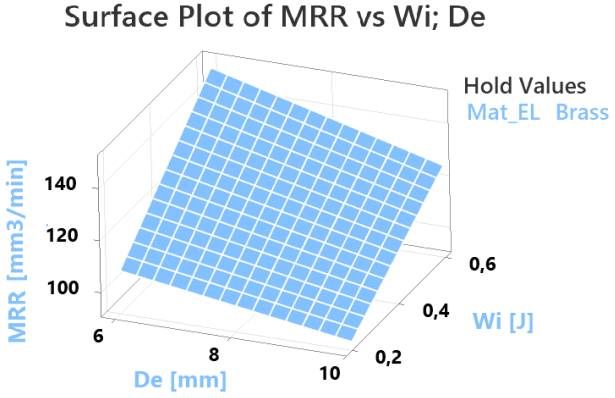

Figure 5. Response surface for MRR (brass electrode)

These visualizations provide comprehensive representation of the functional relationships between process parameters and response variables by systematically varying two independent factors

across their experimental ranges while maintaining remaining parameters at predetermined constant levels. This methodological approach effectively demonstrates individual factor effects, interactive behaviors, and overall response topology within the experimental domain.

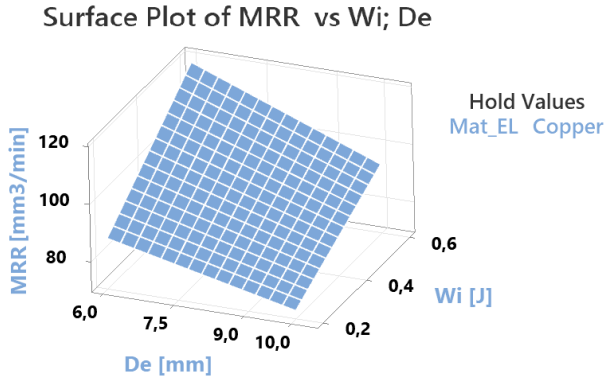

Figure 6. Response surface for MRR (copper electrode)

To obtain a simplified and more easily interpreted perspective of the relationship between the influencing factors and the process outcome, constant-level curves are plotted. To create a level curve, a constant value of the response function is selected (e.g., 90 mm³/min), and all points on the response surface (3D) that have the selected value (90 mm³/min) are projected onto the plane (2D) defined by the W_i and D_e axes. Contour plots for the brass and copper electrodes are shown in Figures 7 and 8, respectively.

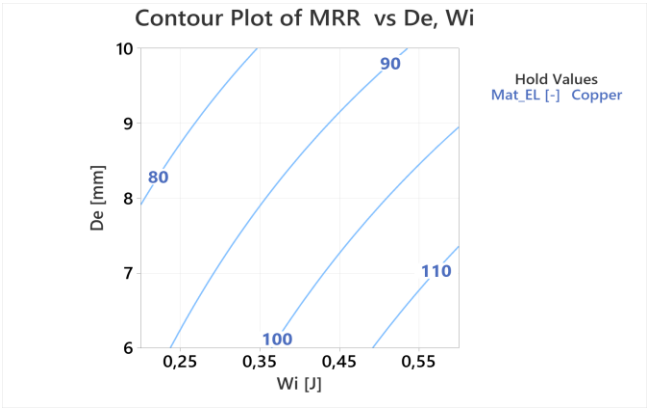

Figure 7. Contour plots for MRR (copper electrode)

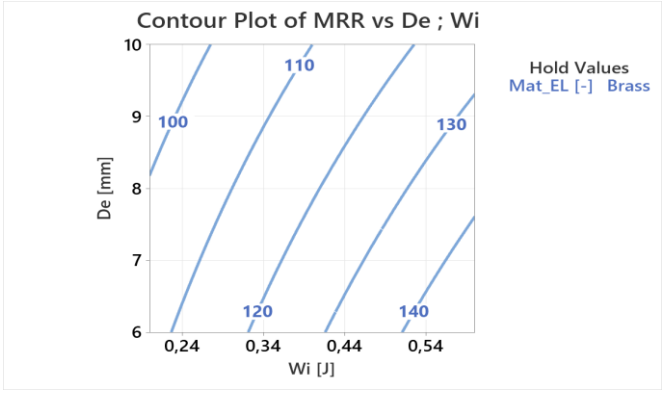

Figure 8. Contour plots for MRR (brass electrode)

3.3 Analysis of the Tool Wear Rate TWR

The impact of the chosen input parameters on the TWR is illustrated in Figure 7. It can be observed that an increase in impulse energy, W_i, results in a corresponding increase in the TWR. A higher-energy pulse generates a superior temperature and pressure in the plasma channel. Although most of the energy is directed toward the workpiece, a significant portion of it also affects the electrode's surface. A higher temperature causes more intense melting and vaporization of the material from the electrode tip.

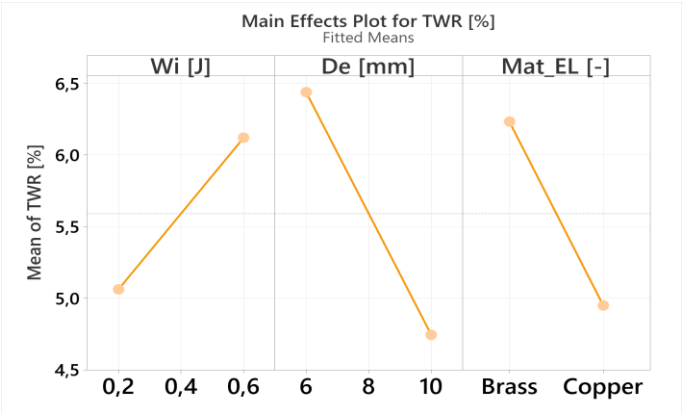

Figure 9. Main effects plot for TWR

An increase in electrode diameter results in a decrease in the TWR, as shown in Figure 9. A plausible explanation is that, for an electrode with a 10 mm diameter, the discharge energy is distributed across a larger contact area. Consequently, the current density decreases, which reduces the intensity of the erosion process on the electrode surface, leading to a lower TWR.

Compared to copper electrodes, brass electrodes are characterized by an increased TWR (Figure 9). The electrical and thermal conductivity of brass is lower than that of copper. As a result, the heat generated during the electrical discharge is not dissipated as efficiently. This leads to a higher concentration of thermal energy in the erosion zone, intensifying the melting and vaporization process.

Table 4 summarizes the regression coefficients derived from the software analysis, providing a comprehensive assessment of how the three selected factors, along with their interactions, influence the tool wear rate (TWR).

Table 4. Calculated values of regression coefficients for TWR

Coeff.	Value	Coeff.	Value
b_0	5,591	b_{12}	0,016
b_1	0,529	b_{13}	-0,026
b_2	-0,846	b_{23}	-0,211
b_3	-0,799		

The ANOVA analysis demonstrates that all individual process factors significantly influence tool

wear rate (TWR), with p-values below 0.05 at the 95% confidence level (Figure 10). Conversely, interaction effects exhibit statistical insignificance with p-values exceeding 0.05, indicating minimal contribution to model variance. Consequently, these non-significant interaction terms can be eliminated from the empirical regression model without compromising predictive accuracy, thereby simplifying the mathematical representation while preserving essential parametric relationships.

Source	DF	Adj SS	Adj MS	F-Value	P-Value
Model	7	19,1573	2,73676	25,49	0,038
Linear	3	13,0697	4,35658	40,58	0,024
Wi [J 10-3]	1	2,2366	2,23661	20,83	0,045
De [mm]	1	5,7291	5,72911	53,37	0,018
Mat_EL [-]	1	5,1040	5,10401	47,54	0,020
2-Way Interactions	3	0,3646	0,12155	1,13	0,501
Wi [J 10-3]*De [mm]	1	0,0021	0,00211	0,02	0,901
Wi [J 10-3]*Mat_EL [-]	1	0,0055	0,00551	0,05	0,842
De [mm]*Mat_EL [-]	1	0,3570	0,35701	3,33	0,210
Curvature	1	5,7229	5,72292	53,31	0,018
Error	2	0,2147	0,10736		
Lack-of-Fit	1	0,2145	0,21451	1072,56	0,019
Pure Error	1	0,0002	0,00020		
Total	9	19,3720			

Figure 10. ANOVA for TWR

The factor hierarchy, derived from their relative influence, demonstrates that electrode diameter constitutes the most dominant parameter, while electrode material ranks second in importance (Figure 11).

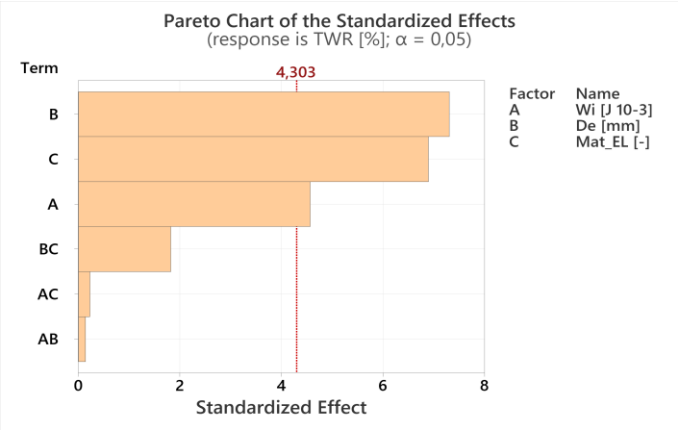

Figure 11. Hierarchy of factors effects for TWR

An empirical model was developed for the fitted models, incorporating only the statistically significant factors and using coded input variables:

TWR= 5,59 + 0,53 Wi - 0,84 De - 0,79Mat_EL(6)

The three-dimensional response surface plots, constructed based on the developed empirical regression model, are systematically presented and analyzed in Figure 12 for the brass electrode configuration and Figure 13 for the copper electrode implementation, respectively.

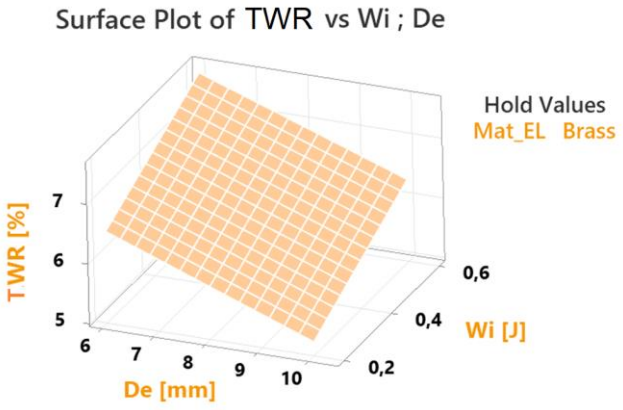

Figure 12. Response surface for TWR (brass electrode)

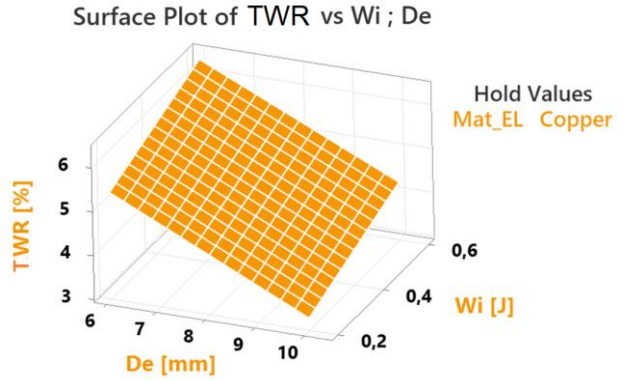

Figure 13. Response surface for TWR (copper electrode)

The constant-level curves for the TWR objective function are presented in Figure 14&15.

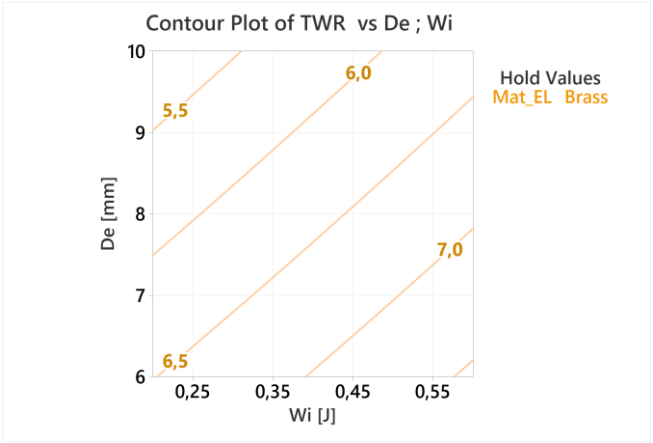

Figure 14. Contour plots for TWR (brass electrode)

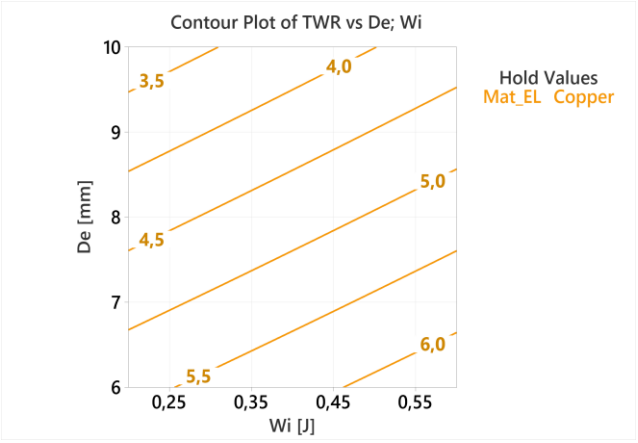

Figure 15. Contour plots for TWR (copper electrode)

3.4 Identification of optimal parameter settings

In experimental research, finding the best configuration of a set of parameters or factors to achieve a specified objective is of particular interest, such as maximizing an outcome (e.g., production rate) or minimizing another outcome (e.g., costs or wear). Based on the experimental data, the Minitab software allowed for the identification of the optimal combination of influencing factors to maximize MRR and minimize TWR (Figure 16). The prediction model identified the optimal combination of parameters (W_i= 0.45 J, D_e = 10 mm) for a brass electrode, which resulted in a MRR of 114.58mm^3/min and an TWR of 5.92%.

Response	Goal	Target
TWR [%]	Minimize	
MRR [mm3/	Maximize	

Multiple Response Prediction

Variable	Setting
Wi [J]	0,457
De [mm]	10
Mat_EL	Brass

Response	Fit	SE Fit	95% CI
TWR [%]	5,919	0,338	(1,631; 10,208)
MRR [mm3/min]	114,58	1,79	(91,80; 137,37)

Multiple Response Prediction

Variable	Setting
Wi [J]	0,6
De [mm]	8,59269
Mat_EL	Copper

Response	Fit	SE Fit	95% CI
TWR [%]	4,986	0,338	(0,690; 9,283)
MRR [mm3/min]	102,24	1,80	(79,42; 125,07)

Figure 16. Identification of optimal parameter settings

For thecopper electrode an optimal combination of input parameters was identified at an impulse energy (W_i) of 0.60J and an electrode diameter (D_e) of 8.59mm. This configuration resulted in a MRR of 102.24mm^3/min and anTWR of 4.98%.

3.5 Investigation on the surface quality

Figure 17 presents images of the EDM processing results, according to the matrix of experiments.The craters resulting from runs 1, 2 and 4, where brass electrodes were used, show surfaces characterized by pronounced irregularities and increased roughness, with poorly defined edges and a non-uniform texture marked by the presence of adherent particles.

Figure 17. Images of the processed workpiece surfaces

The craters obtained in runs 5, 7 and 8, where copper electrodes were used, demonstrate significantly smoother and more uniform surfaces, with better defined and more regular edges, as well as a cleaner texture characterized by the largely absence of material debris and adherent particles.

Figure 18 presents the evolution of the copper electrode in the EDM process, from the initial state to progressive wear.The middle electrode shows signs of moderate wear. Its lower portion, which came into contact with the workpiece, is visibly rougher and darker. Numerous small and medium-sized craters, resulting from repeated electrical discharges, can be observed. The rest of the electrode, above the active zone, remains unaffected.

Figure 18. Images of the copper electrode

The electrode on the right illustrates the effects of advanced electrode wear, a critical aspect in EDM. Its tip is massively eroded, with a rough surface morphology and large, deep craters. This type of degradation reflects a very high TWR, indicating that the volume of material consumed from the electrode is a substantial fraction of the volume of material removed from the workpiece.

Figure 19 shows the brass electrode used in EDM processing, where microscopic crater formation on the surface, carbonized layers, and electrode deterioration can be observed as a result of repeated electrical discharges

Figure 19. Images of the brass electrode

. The electrode exhibits visible signs of erosion in the form of craters, carbon deposits, and surface texture modifications, which are typical results of the electrical discharge machining process. These craters and electrode modifications are inevitable in EDM and directly influence the quality and precision of workpiece machining.

4. CONCLUSIONS

The study demonstrated that impulse energy represents the most influential factor on MRR, with its increase generating more intense plasma channels that efficiently vaporize larger volumes of material per discharge. Reduced electrode diameter and the use of brass instead of copper additionally contribute to increase MRR. Regarding TWR, electrode diameter proved to be the determining factor - smaller diameters and brass electrodes, characterized by inferior electrical and thermal conductivity, produce

significantly higher wear compared to copper electrodes, confirming the importance of electrode material selection in EDM process optimization.

The research established two distinct optimal configurations based on electrode material, with results highlighting significant differences in process behaviour. For the brass electrode, the optimal combination (W_i = 0.45 J and D_e = 10 mm) generated a superior MRR of 114.58 mm³/min, but with higher wear (TWR = 5.92%). In contrast, the copper electrode, optimized at more aggressive parameters (W_i = 0.60 J and D_e = 8.59 mm), produced a lower MRR of 102.24 mm³/min, yet with considerably lower wear (TWR = 4.98%). This comparison demonstrates that while brass offers 12% higher productivity, copper ensures superior electrode durability with approximately 16% less wear, suggesting the need for a differentiated optimization strategy based on process priorities: maximum productivity versus electrode sustainability.

5. REFERENCES

1. Dinesh, S., Vijayan, V., Thanikaikarasan, S., Sebastian, P.J. *Productivity and quality enhancement in powder mixed electrical discharge machining for OHNS die steel by utilization of ANN and RSM modeling*. Journal of New Materials for Electrochemical Systems, Vol. 22, No. 1, pp. 33-43, (2019), doi.org/10.14447/jnmes.v22i1.a07.
2. Gaikwad, M.U.; Krishnamoorthy, A.; Jatti, V.S. *Estimation of Surface Integrity Parameters in Electrical Discharge Machining (EDM) Process—A Review.* In Techno-Societal, Springer Cham, Switzerland, pp. 601–614, (2020), doi: 10.1007/978-3-030-16962-6_61.
3. Boral, S.; Sidhu, S.S.; Chatterjee, P.; Chakraborty, S.; Gugaliya, *A. Multi-response Optimization of Micro-EDM Processes: A State-of-the-Art Review.* In Micro-Electrical Discharge Machining Processes; Springer: Singapore, pp. 293–310, (2019), doi: 10.1007/978-981-13-3074-2_13.
4. Bahgat, M.M.; Shash, A.Y.; Abd-Rabou, M.; El-Mahallawi, I.S. *Influence of process parameters in electrical discharge machining on H13 die steel.* Heliyon, (2019), doi.org/10.1016/j.heliyon.2019.e01813
5. E. Ayhan, S. Güner, M. Yurdakul, and Y. T. İç, *Robust parameter design for EDM-based AL2024-T3 machining,* ournal of Engineering and Applied Science, (2025), doi: 10.1186/s44147-025-00618-8.
6. Barenji, R. V., Pourasl, H. H., &Khojastehnezhad, V. M. *Electrical discharge machining of the AISI D6 tool steel: Prediction and modeling of the material removal rate and tool wear ratio*. Precision Engineering, (2016), doi.org/10.1016/j.precisioneng.2016.01.012.
7. Karthik, S., and Sivakumar Annamalai. *Investigation & analysis of Electrical Discharge Machining on Titanium Diboride Ceramic material with various Electrode materials and dielectric fluids*. Materials Research Express, 2025, doi:10.1088/2053-1591/ada10e.
8. Abu Qudein, J. E., Zaiout, A., Mourad, A. H. I., &Abidi, M. H., &Elkascer, *A. Principles and Characteristics of Different EDM Processes in Machining Tool and Die Steels*. Applied Sciences, 10 (6), 2082, (2020), https://doi.org/10.3390/app10062082.
9. Kuppan, P.; Rajadurai, A.; Narayanan, S. *Influence of EDM process parameters in deep hole drilling of Inconel 718*. Int. J. Adv. Manuf. Technol, 38, 74–84, (2008).
10. Marafona, J.; Wykes, C. *A new method of optimising material removal rate using EDM with copper–tungsten electrodes*. Int. J. Mach. Tools Manuf, 40, 153–164, (2000).
11. Guu, Y.H.; Hocheng, H.; Chou, C.Y., Deng, C.S. *Effect of electrical discharge machining on surface characteristics and machining damage of AISI D2 tool steel*. Mater. Sci. Eng. A, 358, 37–43, (2003), https://doi.org/10.1016/S0921-5093(03)00272.
12. Gubencu, D.V. *Îmbunătățirea continuă a proceselor tehnologice*, Politehnica, Timișoara, Romania, (2023).
13. Montgomery, D.C. *Design and Analysis of Experiments*, 5th ed.; John Wiley and Sons: New York, NY, USA, 2001; pp. 218–276.
14. D. Taloi, *Optimizarea proceselor tehnologice*, Editura Academiei RSR, Bucureşti, (1987)
15. Hinkelmann, K.; Kempthorne, O. *Response Surface Design. In Design and Analysis of Experiments*, Volume 1. Introduction to Experimental Design, 2nd ed.; John Wiley & Sons: New Jersey, USA, pp. 497–531, (2008).